FRACTURE MECHANISM OF PLAIN CONCRETE UNDER UNIAXIAL TENSION

Translation from Transaction of JSCE, No. 466, V-19, 1993

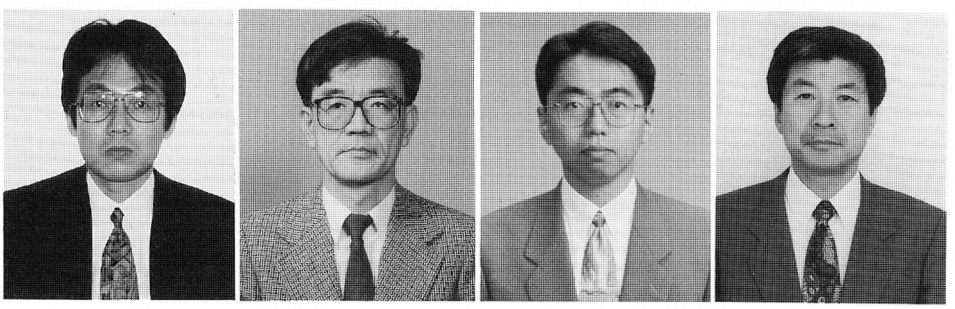

Minoru Ueda Norio Hasebe Masatoshi Sato Hiroaki Okuda

ABSTRACT

Direct tensile tests were carried out on concrete. On the basis of the observed stress-strain (σ-$\in$) curves and observations of the failed sections, the fracture mechanism when concrete reaches its tensile strength under uniaxial loading is discussed. A theoretical elastic analysis is also described; this yields stress singular values in terms of the debonding and cracking fracture mechanism. Fractures which extend outward from the coarse aggregate are considered in particular.

Key words: *plain concrete, fracture mechanism, direct tensile strength, aggregate, crack, stress intensity factor, stress intensity of debonding*

Minoru Ueda, D. Eng., is a member of the Japan Society of Civil Engineers (JSCE); Electric Power Research and Development Center, Chubu Electric Power Co., Ltd. (Kitasekiyama 20-1, Oodakacho, Midori-ku, Nagoya 459)

Norio Hasebe, D. Eng., is a member of JSCE; Professor in the Social Development Division, Engineering Department, Nagoya Institute of Technology

Masatoshi Sato, Eng., is a member of JSCE; Electric Power Research and Development Center, Chubu Electric Power Co., Ltd.

Hiroaki Okuda is a member of JSCE; Manager of Civil Engineering and Construction Section, Electric Power Research and Development Center, Chubu Power Co., Ltd.

1. INTRODUCTION

Many tensile tests on concrete have been reported in the past, and these offer some answers to questions about the factors that affect concrete tensile strength.[1]-[14] As this relates to the aggregate, such factors include the size, separation, grain distribution, roughness, shape, strength of the aggregate itself, and volume, as well as the shape, position, and size of defects on the aggregate surface. Other non-aggregate factors include age, water-cement ratio, specimen length, size of cross section, rate of loading, placed direction, loading direction, and the test method (direct tension, splitting tension, or flexural tension). These factors combine to have a complex influence on overall tensile strength, but it is not certain why some of them have such a qualitative influence. The results of the earlier research mentioned above are widely dispersed; this is a consequence of the various testing conditions used in the work – such as mix proportion, specimen size, and test methods. To clarify the strength characteristics of concrete in more detail, its fracture mechanism needs to be better understood and the effects of these various factors on the fracture mechanism must be discussed.

Concrete fracturing is known to occur when the interface with coarse aggregate begins to peel.[15] Since the progress of this debonding process affects subsequent fracture behavior, and given that aggregate-related factors affecting tensile strength vary over a wide range, clarification of the process by which it occurs at the coarse aggregate interface and of the cracking that results is of great importance. Stress-strain curves (σ-ϵ curves) and observations of failed sections obtained in direct tensile tests offer information of use in elucidating this fracture mechanism. We therefore carried out direct tensile tests and made careful observations of fractures that were attributable to the coarse aggregate. In this report, we also discuss, from the viewpoint of fracture mechanics, the fracture mechanism that determines tensile strength under uniaxial tension. This discussion encompasses various research and test results, including σ-ϵ curves and observations of failed sections, results of direct tensile tests obtained by other researchers, and stress distribution around the aggregate, stress intensity of debonding, stress intensity factor (SIF) of cracks, and energy release ratio in mathematical elastic analysis results obtained by the authors and other researchers. The direct application of linear fracture mechanics to concrete is subject to limitations, since concrete is a compound comprising cement paste and aggregate in a variety of particle sizes. In our research, however, aggregate was modeled such that stress singular values were assigned to phenomenam, including debonding at the coarse aggregate interface and cracks extending from the peeled coarse aggregate into the mortar. These values describe the interface between mortar and coarse aggregate and the mortar itself. This enables linear fracture mechanics to be applied to the concrete. By doing this, the authors demonstrate that the progress of debonding or cracking in a specimen comprising modeled round or rectangular aggregates under uniaxial tension can be qualitatively explained.[16] Interpreted according to Wittmann's "Structure and Mechanical Properties of Concrete,"[17] this categorizes the structural level of concrete mainly as intermediate. Note that this research is restricted in scope to cases where the load is applied monotonously.

2. OUTLINE OF DIRECT TENSILE TESTS

Conventionally, direct tensile tests are usually carried out on specimens measuring less than 10 to 15 cm in diameter and with a maximum coarse aggregate size (Gmax) of less than 20 mm. In our research, we instead adopt samples which are rectangular parallelepipeds 24 x 24 x 12 cm in size containing coarse aggregate with larger Gmax (40 mm). This ensures that fractures extending out from the coarse aggregate can be more clearly observed and allows fractures of different types arising from various aggregate sizes to be readily distinguished (Figure 1). To precisely monitor the behavior of the specimen as a whole and the progress of fracturing of the failed sections, each specimen surface was fitted with 30 mm gauges, as shown in Fig.1, and stress-strain measurements were taken once per 0.12 kgf/cm^2 stress increment. The specimen mixes and test conditions are given in Tables 1 and 2, respectively. The bond test method made use of uniform steel plates and specimen sections.[18] Testing was carried out on three specimens.

In this paper, bond cracks at the coarse aggregate interface are referred to as "debonding," while cracks in the mortar itself are simply called "cracks." The coarse aggregate is referred to as "aggregate."

3. FRACTURE MECHANISM AND TENSILE STRENGTH

(1) Overall behavior of specimens

Average σ-ε curves for each specimen are plotted in Figs. 2 (a) to (c). Tensile fracturing can be described in terms of a correlation between changes in the σ-ε curve and the appearance of debonding and cracking.[15]

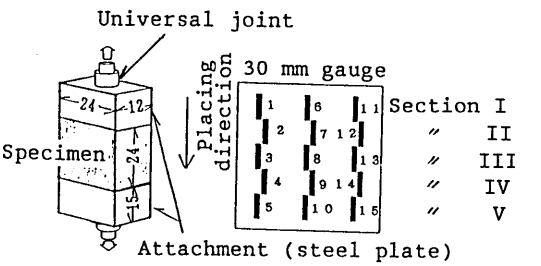

Fig. 1 Direct Tensile Test Equipment and Arrangement of Strain Gauges

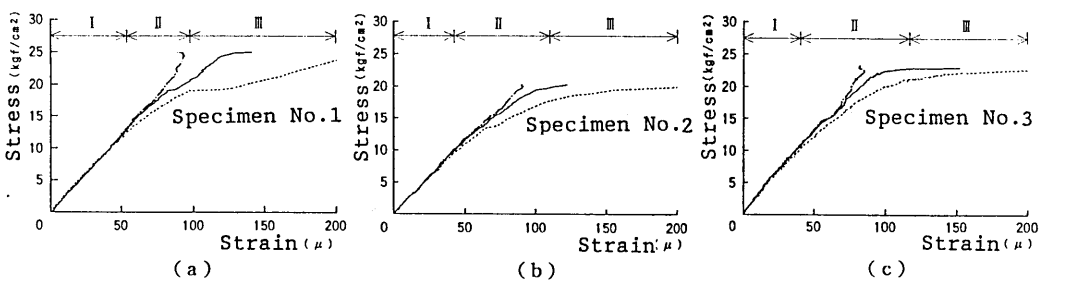

Fig. 2 Average σ-ε Curves of Specimens

Table 1 Mix Proportion of Specimens

Maximum coarse aggregate size (mm)	Water-cement ratio W/C (%)	Fine aggregate ratio s/a (%)	Unit weight (kg/m³) Water W	Cement C	Fine aggregate S	Coarse aggregate G 40~20 mm	20~10 mm	10~5 mm	Total
40	46	43	157	338	783.4	537.0	317.3	169.6	1024.0

Table 2 Testing Conditions

specimens	Three
Age	Bonding agent 2 days
	Specimen 28 days
Loading rate	0.06kgf/cm²/sec (equivalent to splitting test)

The results fall into three regions: elastic behavior (Region I), the non-linear range where debonding occurs (Region II), and the range in which cracks occurred and the curves shift sideways (Region III). These regions can be seen in Fig. 2. Comparison of average σ-ϵ curves of non-failed sections with average σ-ϵ curves of failed sections (Specimen No. 1 and 3 fail at Section II and Specimen No. 2 at Section V) discloses that average σ-ϵ curves of non-failure sections can be represented by an almost linear line, indicating elastic deformation, and that the average σ-ϵ curves of failure-sections begins to curve slightly at the point when the tensile stress reaches about 50% of tensile strength and has deviated considerably by the time peak loading is reached. Figure 3 shows strain distribution of Specimen No. 2 at each load level. The strain distribution is uniform initially, but as loading exceeds a certain level, substantial strain arises at the points which will later become failure sections. This demonstrates that tensile fracturing is localized.

(2) Debonding at aggregate interface

Ordinary aggregate is harder than the mortar surrounding it, and has a modulus of elasticity several times greater than that of mortar.[19] Thus, tensile stress appears in the aggregate at a position roughly in line with where the tensile load acts. This has been verified by a stress analysis of circular and elliptical elastic inclusions as well as rigid rectangular inclusions. The stress concentration intensifies, for elliptical inclusions, as the radius of curvature becomes smaller.[20]-[22] In the case of rectangular inclusions, it intensifies as the solid angle at the position facing the tensile load becomes smaller[23] and as the inclusions become harder than the base material.[21]-[23] In actual concrete, debonding occurs at the point on the aggregate interface that is most vulnerable in terms of stress because of aggregate size and shape; that is, it is related to the solid-angle, radius of curvature, unevenness of bonding strength, and loading direction where stress tends to concentrate. Voids caused by bleeding and which exist in the concrete before loading, or initial defects related to non-bonding at the aggregate interface frequently trigger fractures. In actual samples, traces of separated aggregate are observed in the failed section after tensile testing.[1],[5],[12],[26],[27] Fenwick et al published the results of observations of the dependence of failure on the orientation of concrete placement and the direction of the tensile load.[5] According to their work, when the orientation of concrete placement and of acting tensile load line up (and it is noted that bleeding occurs on the lower surface of the aggregate opposite the tensile load in such cases, indicating that aggregate and mortar are not fully bonded), most aggregate in the failed section remains bonded to the bleeding-free upper face of the failed section. On the other hand, when the orientations are perpendicular (in this case, the tensile loading and bleeding on the lower surface of the aggregate almost line up), the aggregate bonds almost equally to the upper and lower faces of the failed section. Photo 1 shows the failed faces of a specimen in the authors' experiments. Table 3 gives the ratio between aggregate debonding on the upper surface and on the lower surface at failed sections. More than 80% of aggregate debonding occurs at the lower face. Table 4 lists the area of aggregate debonding at the interface as observed in failed sections in order peeled area. Relatively large aggregate, closer in size to Gmax, is found to have peeled. This result reveals that debonding occurs on the side of the aggregate interface facing the tensile load direction if there is insufficient adhesion. It also reveals that fracturing is more likely to occur with larger aggregate which tends to have initial defects such as voids and poor adhesion due to bleeding and which comes under concentrated stress. In cases where the upper surface of the aggregate is found to have peeled away from the mortar, most of the aggregate is relatively large, has an upward taper, and is subject to a stress concentration on its upper surface. Hatta et al.[22] carried out stress analysis on two circular inclusions

of different sizes and with a hardness greater than base material under uniform loading. The authors[24] subjected two rhombic rigid inclusions of different size to stress analysis. Both indicate that the interface with a larger inclusion is more prone to the concentration of tensile tension that causes debonding. Thus, these results suggest that where aggregate particles have the same shape and no initial defects, larger ones are more prone to debonding.

Fracture toughness decreases in the following order: aggregate, mortar, and adhesion between mortar and aggregate.[25] As explained, the stress concentration arising from the presence of aggregate appears at the aggregate interface, leading to debonding at the interface and eventual fracture. Figure 4 (a) shows σ-∈ curves for certain locations in the failed section; the numeral corresponds to the gauge number (Fig. 1). Uniform deformation is observed at all gauges in the failed section under low loading. When the load level reaches a certain value, however, debonding occurs at the aggregate interface. The slope of the results from gauge No. 5 changes slightly at Point A in Fig. 4(a), indicating that debonding occurred.

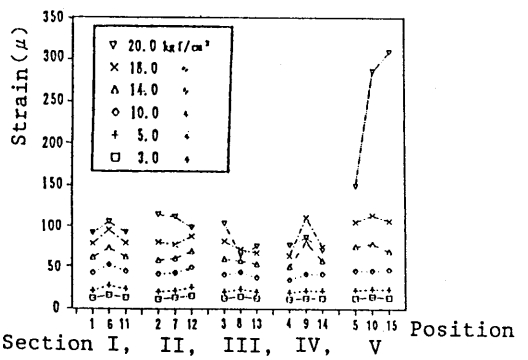

Fig. 3 Strain Distribution of Specimen No. 2 at each load level

Table 3: Ratio of Aggregate Debonding Occurring at Upper Surface to that at Lower Surface

Specimen	Lower surface of aggregate (%)	Upper surface of aggregate (%)
No. 1	77	23
No. 2	88	12
No. 3	94	6

Table 4: Surface Area of Aggregate with Debonding or Fracturing (in order of magnitude)

Specimen	Peeled surface area (cm²)				Fractured surface area (cm²)			
	Max	2	3	4	Max	2	3	4
No. 1	9.9	7.7	4.9	3.2	2.2	2.2	1.4	1.1
No. 2	10.8	6.9	6.4	5.4	2.6	2.3	1.8	0.4
No. 3	12.1	4.7	4.7	3.5	4.5	3.1	3.1	2.4

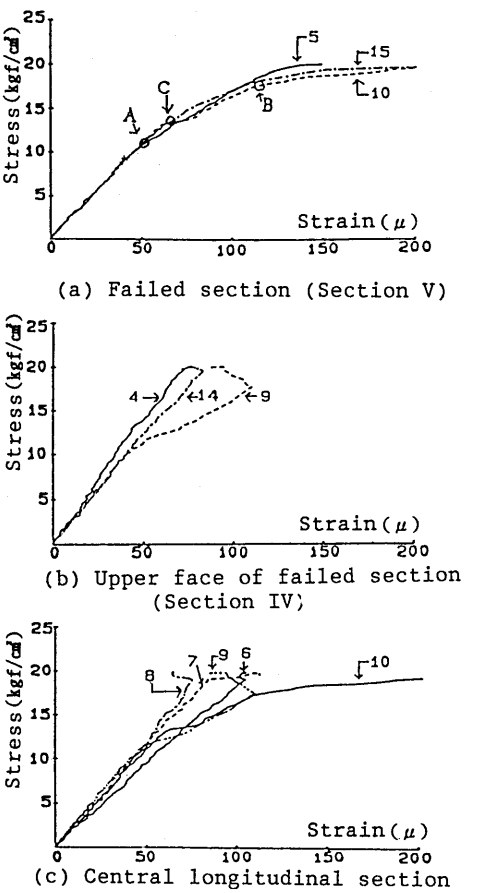

(a) Failed section (Section V)

(b) Upper face of failed section (Section IV)

(c) Central longitudinal section

Fig. 4: Stress-Strain Curves of Sections (Fig.1) of Specimen No. 2

In our experiments, the stress at Point A (expressed as σd) is around $\sigma d/\sigma t = 0.5$ in terms of tensile strength (expressed as σt), as shown in Table 5. Photo 1 shows that the largest aggregate is found near gauge No. 5 and the results from this gauge indicate that the interface of this aggregate peeled the earliest. Figure 4(b) shows that, even though these are not σ-$\in$ curves at failed sections, the plot for gauge No. 9 changes in slope at a load level slightly larger than at gauge No. 5. This may be understood to indicate that some debonding occurs even outside the failed section. No such observation was made with Specimens No. 1 and No. 3.

Table 5: Strain and Stress at Failure Points of σ-$\in$ Curve

Specimen	Point A			Point B			Tensile strength
	Strain εd (μ)	Stress σd (kgf/cm²)	$\frac{\sigma d}{\sigma t}$	Strain εm (μ)	Stress σm (kgf/cm²)	$\frac{\sigma m}{\sigma t}$	σt (kgf/cm²)
No. 1	55	12.7	0.51	94	18.0	0.72	24.9
No. 2	46	10.0	0.50	111	17.5	0.87	20.2
No. 3	46	10.8	0.47	114	19.2	0.83	23.0

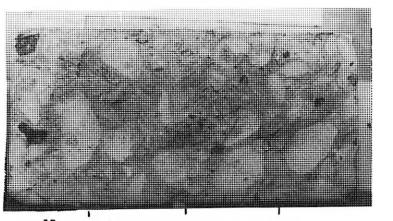

Photo 1: Failed Section

(3) Characteristics of the debonding process

A stress analysis was carried out at the interfaces of circular, elliptical, and rhombic inclusions to investigate the debonding mechanism. Circular or elliptical inclusions may be taken as models of the curved interfaces characterizing aggregate comprising rounded stones, such as river gravel. Rectangular inclusions may be taken as models of the angular and linear interfaces characterizing aggregate comprising crushed stones with angular faces. The results of stress analysis of debonding at the interfaces of these inclusions are used as the basis of a discussion of the characteristics of the debonding process.

Figures 5 and 6 show the stress intensity of debonding for circular rigid inclusions[28] ($|\beta o|$: is the stress intensity of debonding and allows evaluation of the characteristics of the debonding process,[23]) and the stress near the extremity of debonding.[28] The debonding stress curve has the form of an upward convex curve with a maximum (Fig. 5). (In Figs. 5, 6, 8 and 11 - 14, κ is a function of Poisson's ratio ν. For planar strain, it is $3 - 4\nu$. For generalized planar stress, it is $(3 - \nu) / (1 + \nu)$. For mortar, κ is about 2. In Figs. 5, 6, 8, and 10 - 14, values along the y axis are all dimensionless.) For inclusions which are circular elastic body or elliptical rigid body, the stress singular value at the extremity of debonding has peaks.[29]-[31] Stress in the normal direction near the extremity of debonding are in tension and peaks at around $\theta = 50°$ when there is little debonding. Before this peak, the stress increases monotonously and, thereafter, decreases monotonously and changes in compression. The absolute value of shear stress increases monotonously as debonding progresses, with a peak at around the point when the stress in the normal direction changes in compression, and then subsequently decreases (Fig. 6). This is because the direction of the debonding process gradually moves toward the direction of the load. As a result, although the fracture conditions of the debonding process must be defined, where there are curved aggregate interfaces debonding progresses even without additional load when the load reaches the fracture toughness value for the debonding process. Thereafter, debonding progresses stably as the load increases, but this progress is gradually upset as the direction of the debonding process change. Saito et al[32] carried out direct tensile testing of concrete including round model aggregate (ϕ = 3.2 cm) and confirmed that debonding began somewhere at the interface and finally caused fracture of the specimen (Fig. 7).

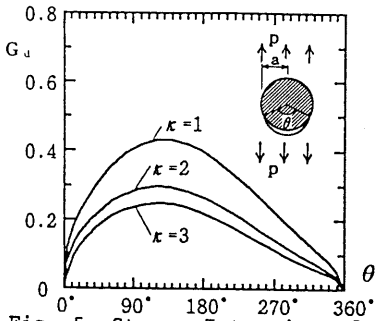

Fig. 5: Stress Intensity of Debonding at Circular Rigid Inclusion[28]

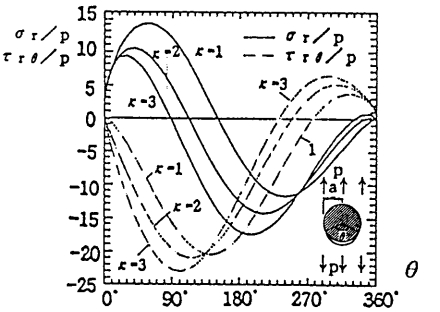

Fig. 6: Stress near Extremity of Debonding at Circular Rigid Inclusion[28](σr:stress in normal direction,τr:stress in shear direction)

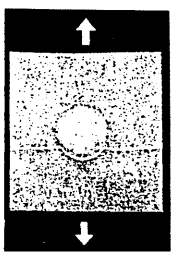

Fig. 7: Fracture Condition of Specimen in Direct Tensile Test using Round Model Aggregate

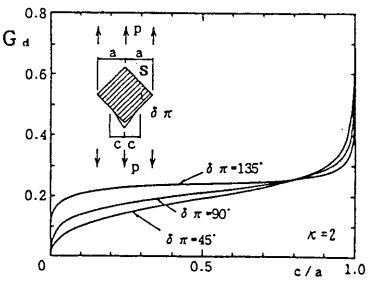

Fig. 8: Stress Intensity of Debonding at Rhombic Rigid Inclusion[23]

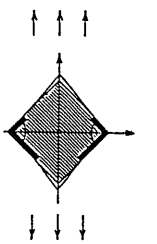

Fig. 9: Rigid Symmetrical Rhombic Inclusion with Two Asymmetrical Areas of Debonding

In the case of rhombic inclusions, stress intensity of debonding increases monotonously (Fig.8).[23] This is because the direction of the debonding process and load do not change as debonding proceeds. The authors have studied the characteristics of debonding in the case of rhombic rigid inclusions under uniform tensile loading (Fig. 9) in terms of the stress intensity of debonding.[33] The inclusions were symmetrical in shape and two asymmetrical occurrences of debonding were seen. The study shows that as debonding on one side proceeds, the debonding stress on the other side shows a gentle monotonous decline. The same observation applies when inclusions are circular elastic body[29] or ellipitcal rigid body.[31] When debonding is aggravated on either side, the debonding stress on that side intensifies. This indicates that when debondings are observed on both sides, it begins for some reason on one side and then spreads over the whole of that side. At this time, debonding develops little on the other side. For a rigid rhombic inclusion under uniform tensile loading and with debonding on one side (Fig. 8), the stress intensity at solid angle with no debonding (Point S) monotonously increases as debonding develops on that side. This indicates that debonding is unlikely to begin within this solid angle.[23] The stress intensity at Point S is a value indicating the level of the stress singularity within the solid angle and allows evaluation of the likelihood of debonding. These results were obtained for aggregate with a symmetrical shape. In the case of the more typical asymmetrical aggregate, the earlier phenomenon above – that is debonding developing outward from one spot – is thought to be more likely to occur. Consequently, where the aggregate has linear interfaces and solid angles, once debonding appears at one point, it moves to the next solid angle with no additional load and from there spreads to another solid angle when the load reaches a certain level. Debonding, however, may not develop when the interface and load are in certain directions.

In summary, once debonding begins to develop, whether the interface is curved or linear, it immediately affects a certain area of the aggregate interface. Debonding develops both as the load rises and due to interference resulting from the debonding process itself. The latter will be discussed later. However, if debonding develops such that its direction of progress changes with respect to the load direction, it will only spread with difficulty.

(4) Mutual interference and the development of debonding

The initiation of debonding at the aggregate interface and its subsequent development does cause the base material, mortar, to crack.
This is because, as discussed earlier, the fracture toughness value of mortar is greater than that of the bond between mortar and aggregate. Consequently, as the load increases, debonding is initiated and then develops along the interface rather than growing out from where it first appears. Since the initial location is very influential, subsequent debonding tends to break out nearby at points where the stress is more concentrated. With increasing load, this debonding further develops and expands until it interferes. In Fig. 4 (a), the debonding occurs at interfaces near gauge No. 5 (Point A) and has an influence on gauge No. 10; this gauge's σ-ϵ curve then indicates a clear break point (Point C). This demonstrates that debonding also occurred near gauge No. 10, and consequently the σ-ϵ curves of gauges No. 5 and 15 have a smaller slope. This figure further shows the slope of the σ-ϵ curves gradually becoming less as debonding at the interfaces develops under increasing load. While the average σ-ϵ curves (Fig. 2) have a gently curved, non-linear shape, the curves shown in Fig. 4 (a) are taken from failed sections. These curves come about because the average σ-ϵ curve indicates debonding on aggregate interfaces occurs and develops continually to some extent. On the other hand, the σ-ϵ curves at various locations on failed sections indicate that the occurrence of debonding at some aggregate interfaces was followed by interacting peeling at other interfaces. The peeled portions interfere with each other and, once initiated, expand over a certain range without any additional load.

Debonding generally develops to a size around that of the aggregate and is not uniform in scale. It also occurs on other aggregate interfaces near the same section. Mutual interference areas of debonding may be inferred from the interference in stress intensity factors (SIF). Values of SIF for two cracks of the same length, three cracks of the same length (Fig. 10), an infinite number of cracks of the same length (Fig. 10), and two cracks of different lengths were obtained.[34] Ignoring the knowledge that debonding actually takes place at the aggregate interface and instead adopting the approximate assumption that debonding is a form of cracking that takes place in a uniform elastic body, it is found that incidents of debonding separated by a clearance up to about 10 times the length of each crack interfere with each other. (For example, the influence of interference is lost at around 2a/d = 0.1 in Fig. 10.) In reality, debonding at aggregate interfaces does not always occur in the same failure section. However, according to the result of analysis of SIF of cracks running parallel to each other but on different lines, the

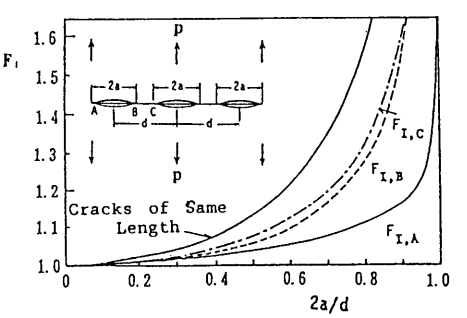

Fig. 10: Stress Intensity Factors due to Interference between Cracks of Same Length[34] (F_{IA}, F_{IB}, and F_{IC} are stress intensity factors at Points A, B, and C, respectively, for the three equal-length cracks shown in the figure.)

degree of interference of two cracks separated in vertical and lateral directions by a clearance equal to the length of the crack is known to be equal to that of cracks on the same line and with a clearance in the lateral direction.[34]

(5) Cracking

Figure 4 (a) shows how the σ-ε curves shift considerably sideways after Point B. Figures 4 (b) and (c) show σ-ε curves obtained from a strain gauge in a section (Section IV) just above the failed section and from gauges on a longitudinal section through the center of the specimen, respectively. After the stress exceeds a level corresponding to Point B, the strain tends to decrease. This indicates that cracking takes place at Point B and that the strain is concentrated in the failed section (Section V) as the fracture progresses. Zaitsev[35] used model concrete containing various sizes of large round aggregate to simulate the phenomena of debonding, cracking, and crack propagation; σ-ε curves resulting from his simulations were published. His results reveal that the σ-ε curves are linear until the aggregate surfaces begin to peel, and that the curves become slightly non-linear once debonding has developed, then shifting sideways as cracking occurs.

The strain on failed sections when cracking occurred turned out to be almost the same for all three specimens, ranging from 94 to 114 μ, as shown in Table 5. Table 6 arranges strain values in a more easily understandable form, based on the supposition that mortar cracks when the σ-ε curve obtained from direct tensile tests by other researchers begins to shift sideways (which corresponds to Point B in Fig. 4 (a)). The results given in Table 5 are also integrated into Table 6. The values fall within the range 80 to 120 μ regardless of mixing differences. Yoshimoto[38] conducted direct tensile tests and carried out microscope studies of mortar slices taken from the specimen, revealing that the value of strain at which the σ-ε curve begins to lose linearity correlates well with the point at which paste cracking begins to grow substantially. This value is 80 μ according to his study. Similar results have been observed in other specimens subjected to mortar flexural tests.[39] Table 7 tabulates Yoshimoto's results along with values of strain at which the σ-ε curve begins to lose linearity as obtained by the authors and other researchers.

These results indicate that the value of strain at which mortar begins to fracture and cement paste fracturing becomes serious is around 60 to 80μ, although this varies according to the exact mortar mix. The results then show that this value range agrees with the fracture toughness of the mortar as expressed by strain. Comparing the strain values in Tables 6 and 7, those in Table 6 are generally larger. Although the mortar mix proportion, test method, specimen size, and measuring gauge length and positions are the same in Yoshimoto's tests, strain in Table 6 is larger than that in Table 7. From these results, it can be deduced that the strain when mortar cracks form is greater

Table 6: Strain Values at the Time of Mortar Cracking in Direct Tensile Tests of Concrete

Researcher	Strain μ	Mix proportion Water : Cement : Fine aggregate : Coarse aggregate	Gmax mm
Yoshimoto[7]	110	0.59 : 1.00 : 2.57 : 2.43	25
Hatano[1]	About 110 **	0.37 : 1.00 : 1.84 : 3.41	25
	120 〃	0.50 : 1.00 : 2.37 : 4.21	
	80 〃	0.65 : 1.00 : 3.55 : 5.80	
Watanabe[27]	110	0.50 : 1.00 : 1.91 : 2.59	*
Author (in Table 5)	94～114	0.46 : 1.00 : 2.32 : 3.03	40

* Not given in literature

** Approximate because these figures cannot be identified from the results given in the literature

Table 7: Strain Values at Which σ-ε Curves Begin to Lose Linearity in Direct Tensile Test of Mortar

Researcher	Strain μ	Mix proportion Water : Cement : Fine aggregate
Yoshimoto	80	0.59 : 1.00 : 2.57
Hatano[1]	60	0.50 : 1.00 : 3.00
Gopalaratnam[10]	80	0.45 : 1.00 : 2.00
Authors	70	0.52 : 1.00 : 2.75

than the strain corresponding to mortar fracture toughness since it includes the strain due to debonding at aggregate interfaces. The results also tell us that the strain at the extremity of debonding has reached the mortar fracture toughness and this is where cracks are initiated.

The authors analytically investigated the possibility of cracks being initiated from the extremity of debonding on circular rigid inclusions. This indicated that since the normal stress near the extremity of debonding switches from tensile to compressive when debonding takes place at around 100° in angle of circumference, debonding only develops with difficulty (Fig. 6). Cracking is most likely to occur as a result of the energy release ratio of crack (Fig. 11) and SIF for Mode I (Fig. 12) have peaks.[28] These results are in good agreement with the actual positions of cracks being initiated (around 100° in angle of circumference) obtained in tests by Saito et al.[32] (Fig. 7) For angular aggregate, debonding grows until it reaches the solid-angle point, as discussed earlier. The solid angle then changes its characteristics: from a solid angle formed at bonded aggregate interfaces to one formed at interface where it is freed from stress by debonding along with interface and interface where the aggregate remains bonded. As a result, the stress intensity increases in a stress field near the solid-angle, and cracking is very likely to take place.[23]

In summary, as the load increases, more debonding occurs at aggregate interfaces and each point of debonding grows, thus increasing the amount of mutual interferences. Finally, cracks occur at the extremity of debonding on the aggregate interface. Aggregate at which cracking begins is not necessarily that at which debonding initiates. Rather, cracking occurs at peel points whose tips are under the greatest stress concentration and which reach the mortar fracture ductility first. The degree of stress concentration at an extremity is determined by the size of the peeled area on the aggregate interface, the degree of interference from neighboring debonding, and the direction of debonding and the tensile load. Table 8 shows the condition of the failed sections and the stress at Point B (expressed in σm). This reveals that Specimen No. 2, which has a larger area of peeled aggregate than the others, has the smallest σm. This is because the larger amount of debonding in Specimen No.2 caused mutual interference and affected the specimen, eventually reducing the load level at which cracking occurred.

(6) Condition of failed section and tensile strength

Carino et al.[40] took x-rays of fractured specimens containing round model aggregate, noted that cracking was not visible around critical cracks, and concluded that growth of the initial cracks caused final failure. In our experiment, no case of a sideways shift in the σ-ϵ curve was seen (Figs. 4 (b) and (c)). Such a shift is usually associated with cracking at a failure section. Thus these test results indicate that where initial cracking occurs, the failure is likely to occur.

The authors analyzed the SIF of cracks[28] formed at the solid angle of rigid rhombic inclusions with debonding on one side and at the corner of rhombic holes[41] (Fig.13). (Holes and rigid inclusions correspond to two extremes of rigidity; ordinary elastic inclusions are categorized as lying between them.) According to our results, when an inclusion is harder than the base material, the SIF of a crack formed at the solid angle takes a minimum value when the crack is much shorter than the size of the inclusion. SIF monotonously increases with crack length beyond that. In this case, where the inclusion is single and rhombic, the cracks are shown to grow unstably. When a crack nears a circular inclusion that is harder than the base material, its SIF decreases under certain loads (Fig. 14).[42] But when there are debondings at the circular inclusion and those debondings have grown larger than a certain size, this reduction in SIF slows down. With larger

debonding, SIF increases. As the crack moves closer to a circular inclusion, the stress intensity at the extremity of the debonding increases.[30] These results allow us to conclude that for relatively severe debonding of the aggregate interface, a crack formed at the extremity of the debonding on the aggregate interface causes further debonding growth as it approaches other aggregate and peeled areas begin to crack. Eventually, the peeled sections or cracks connect up with other cracks without additional loading. This is why the σ-∈ curves shift sideways after crack formation (Fig. 4 (a)). This understanding corresponds to the

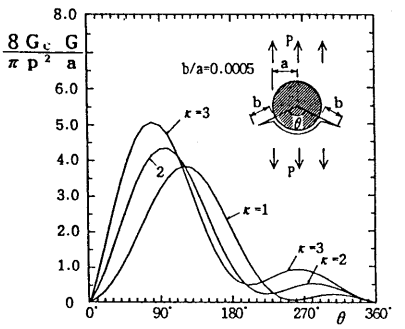

Fig. 11: Energy Release Ratio of Cracking from Circular Rigid Inclusion[28] Gc (G: modulus of shear elasticity)

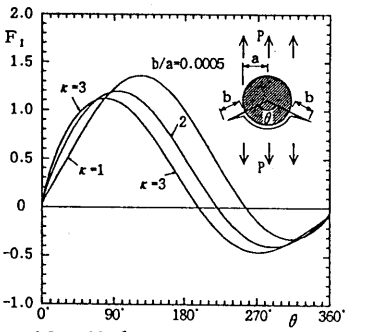

Fig. 12: Mode I Stress Intensity Factors of Cracking from Circular Rigid Inclusion[28]

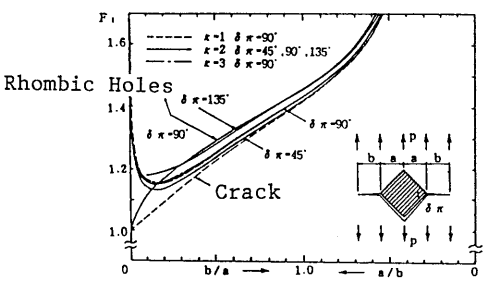

Fig. 13: Mode I Stress Intensity Factors of Crack Occurring from Rhombic Rigid Inclusion with Debonding and from Rhombic Holes[23] $F_I = K_I/(p\sqrt{\pi a})$

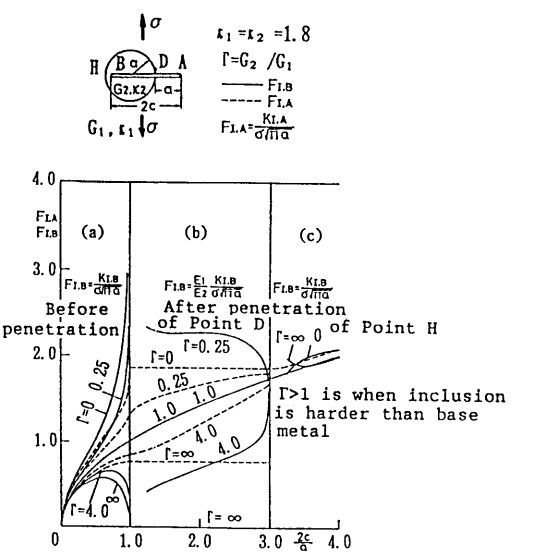

Fig. 14: Stress Intensity Factors of Crack Approaching and Penetrating Inclusion[42] (F_{IA} and F_{IB} are stress intensity factors at Point A and B, respectively, as shown in the figure)

Table 8: Condition of Failed Section and Tensile Stress

Specimen	Peeled aggregate area ratio (%)	Fractured aggregate area ratio (%)	Stress (kgf/cm²)	σt−σm (kgf/cm²)
No. 1	23	5	18.0	6.9
No. 2	34	2	17.5	2.7
No. 3	25	8	19.2	3.8

observations discussed earlier; traces of lost aggregate are seen on one side of the failed section after tensile fracture[1],[5],[12],[26],[27] and traces of aggregate with the largest particle size or thereabouts are found in failed sections in our test (Table 4). This happens because, as explained in (2), debonding is more likely to occur and expand, and cracking is more likely to arise, if the aggregate is larger, due to bleeding and concentration of tensile stress.

After crack formation, strength intensification is observed. The ratio of stress at initial cracking σm to tensile strength σt, $\sigma m/\sigma t$, is 72% to 87% in our study (Table 5). Other researchers have found it to be around 70% (Hatano,[1]) around 95% (Yoshimoto[7] and Watanabe[37]), and about 75%. (Slate[15]) According to these observations, since areas of debonding connect up without additional loading, there must be another mechanism causing strength intensification after cracking. On the other hand, aggregate fracturing is seen in the failed section in tensile testing.[1],[11],[27] In our test, aggregates smaller than those suffering debonding were subject to fracturing (Table 4). To identify dependence on aggregate size, the authors conducted direct tensile tests[18] on 30 cm cylindrical specimens each containing aggregate with a maximum particle size of 150 mm. This specimen size was chosen to offer a wider range of aggregate sizes. In these tests, aggregate of the maximum particle size or close to it suffered debonding at the interface, as seen in the failed sections. Aggregate of smaller particle size – that is, around 40 mm – was found to be fractured. The fracture toughness of the aggregate is significantly greater than that of mortar, yet it is not that the aggregate itself fractures, but rather a crack develops toward the aggregate and finally fractures it. As mentioned above, because peeled sections are likely to join with cracks when debonding at the interface is relatively severe, fractured aggregate has little or no debonding. Such aggregate particles are smaller than a certain size, as indicated by the test results above, since larger aggregates are more likely to peel (See (2)). Since the fracture toughness of the bond between mortar and aggregate is low, it appears difficult for aggregates which have no debonding or little debonding to be present. However, given the observed fact that some aggregate does fracture, there must be cases where the formation and growth of debonding is inhibited, depending on the size and shape of the aggregate and degree of bonding between the aggregate and mortar.

When a crack approaches a circular inclusion which is harder than the base material and has little or no debonding, the SIF of the crack decreases under a certain load.[42],[30] This situation corresponds to around $2c/a = 1.0$ when Γ is one or greater in the domain (a) in Fig. 14. Results of analysis indicate that cracks stretching toward aggregate with little or no debonding are blocked by the aggregate. The arrival of a crack at an aggregate particle does not immediately cause the aggregate to fracture, because fracture toughness is significantly greater than that of mortar. Under these conditions, cracks reach some aggregate interfaces as the load increases. The extremities of cracks that have reached aggregate particles may possibly cause the aggregate interfaces to peel, which would eventually remove such aggregates. However, debonding is considered less likely to occur under certain orientations of the interface which a crack reaches and directions of tensile loading. The crack then stops at the aggregate particle it reaches.

When the increasing load causes the crack extremity, which is in contact with the aggregate, to reach aggregate fracture toughness, the aggregate begins to fracture. When a crack penetrates a circular inclusion that is harder than the base material, the SIF of the crack increases rapidly and monotonously as compared with when there is no inclusion. As the crack penetrates the inclusion, its SIF closes on the value when there is no inclusion, since the inclusion has only a small influence. (See domains (b) and (c) in Fig. 14). This indicates that once a crack exceeds the

fracture toughness of the aggregate and moves into the aggregate, the fracture develops unstably through the aggregate. This phenomenon, then, affects cracks that have already reached other aggregate particles by that time or are growing toward them. It causes a chain reaction and their SIF intensifies, finally resulting in fracture of some of the aggregate particles. Once the aggregate begins to fail, fractured sections of aggregate join up with already formed broken sections, causing extremely unstable fractures which instantly result in failure of the entire specimen. From this, it may be deduced that the moment at which aggregate fracturing begins would correspond to the tensile strength of the specimen. The increment in loading after cracking is affected by the actual load level at which cracking occurs, the distribution of debondings before cracking occurs, and the location, size, and hardness of debonding-free aggregate particles. For example, if a large amount of debonding has occurred before cracking starts, failure sections tend to be formed and little extra loading is possible because there are fewer cracks that expand to aggregates which have no or small debonding. In Table 8, the strength intensification after cracking ($\sigma t - \sigma m$) is the smallest for Specimen No. 2, which has the greatest ratio of peeled aggregate area and the smallest ratio of fractured aggregate area. This observation bears out the understanding deduced above.

4. CONCLUSION

Direct tensile tests of concrete have been carried out to look into the tensile fracture mechanism of plain concrete. Stress-strain curves, fracture characteristics, and other results obtained from the tests were used, along with stress analysis based on mathematical elastic theory and analysis of stress singular values such as stress intensity factor and stress intensity of debonding in fracture mechanics, to investigate the fracture mechanism. In summary, it can be said that fracturing to the tensile strength of the concrete occurs after a series of events. First, some aggregate interfaces peel and these peeled areas develop until they interfere with one another. This finally leads to cracking. These cracks, together with already existing peeled areas of the aggregate interface, lead to further cracks and debonding due to mutual interference. More cracks result from debonding on other aggregate interfaces and these too develop. As these cracks join with peeled sections, they extend toward other aggregate particles, and the aggregate fractures as if in a chain reaction. This finally leads to failure of the concrete.

References

[1] Hatano, M.: Dynamical Behaviours of Concrete under Impulsive Tensile Load, Proceedings of the Japan Society of Civil Engineers, No.73, pp.23 to 34, 1961.

[2] Spetla, Z. and Kadlecek, V.: Effect of the Slenderness on the Direct Tensile Strength of Concrete Cylinders and Prisms, BULLETIN RILEM, No.33, pp.403-412, 1966.

[3] Kadlecek, V. and Spetla, Z.: Effect of size and Shape of Test Specimens on the Direct Tensile Strength of Concrete, BULLETIN RILEM, No.36, pp.175-184, 1967.

[4] Johnston, C.D.: Strength and Deformation of Concrete in Uniaxial Tension and Compression. Magazine of Concrete Research, Vol.22, No.70, pp.5-16, 1970.

[5] Fenwick, R.C. and Sue, C.F.C.: The Influence of Water Gain upon the Tensile Strength of Concrete. Magazine of Concrete Research, Vol.34, No.120, pp.139-145, 1982.

[6] Saito, M. and Imai, S.: Direct Tensile Fatigue of Concrete by the Use of Friction Grips, ACI Journal, September-October, pp.431-438, 1983.

[7] Yoshimoto, A., Hasegawa, H., and Kawakami, M.: Relation between Direct Tensile Strength, Splitting Tensile Strength and Modulus of Concrete and Mortar, Cement & Concrete, No.435, pp.42-48, 1983.
[8] Ditommaso, A.: Evaluation of Concrete Fracture, Fracture Mechanics of Concrete, ed. by Carpinteri, A. and Ingraffea, A.R., Martinus Nijhoff Publishers, pp.31-65, 1984.
[9] Raphael, J.M.: Tensile Strength of Concrete, ACI Journal, March-April, pp.158-165, 1984.
[10] Gopalaratnam, V.S. and Shah, S.P.: Softening Response of Plain Concrete in Direct Tension, ACI Journal, May-June, pp.310-323, 1985.
[11] Tinic, C. and Brühiwiler, E.: Effect of Compressive Loads on the Tensile Strength of Concrete at High Strain Rates, The International Journal of Cement Composites and Lightweight Concrete, Vol.7, No.2, pp.103-108, 1985.
[12] Guo, Z. and Zhang, X.: Investigation of Complete Stress-Deformation Curves for Concrete in Tension, ACI Materials Journal, July-August, pp.278-285, 1987.
[13] Xie, N. and Liu, W.: Determining Tensile Properties of Mass Concrete by Direct Tensile Test, ACI Materials Journal, May-June, pp.214-219, 1989.
[14] Nagayama, I. Watanabe, K. and Ohata, N.: Discussions on a Direct Tensile Strength Test of Concrete for Dams and Test Results, Engineering for Dams, No.54, pp.38-46, 1991.
[15] Slate, F.O. and Hover, K.C.: Microcracking in Concrete, in Fracture Mechanics of Concrete Material Characterization and Testing, ed. by Carpinteri, A. and Ingraffea, A.R., pp.137-159, 1984.
[16] Ueda, M., Higashigawa, T., Hasebe, N., and Umehara, H.: Study on Fracture Mechanics of Internal Behavior Attributable to Coarse Aggregate of Concrete for Dam, Proceedings of the 46th Annual Conference of the Japan Society of Civil Engineers, V-244, pp.504-505, 1991.
[17] Wittmann, F.H.: Structure and Mechanical Properties of Concrete, Concrete Journal, Vol.21, No.3, pp.19-30, 1983 (translated by Hirozo Mihashi).
[18] Sato, M., Ueda, M., Endo, T., and Hasebe N.: Study on Attachment for the Direct Tensile Test of the Large Size Concrete Specimen, Proceedings of the Japan Concrete Institute, Vol.14, No.1, pp.549-554, 1992.
[19] Kawakami, H.: Influence of Aggregate Type on Concrete Mechanical Behavior, Proceedings of the Japan Concrete Institute, Vol.13, No.1, pp.63-68, 1991.
[20] Murakami, T. and Shimizu, M.: Effects of Nonmetallic Inclusions, Small Defects and Small Cracks on Fatigue Strength of Metals, Transactions of the Japan Society of Mechanical Engineers (Version A), Vol.54, No.499, pp.413-425, 1988.
[21] Hasegawa, H. and Kumamoto, K.: Stress Concentration of a Strip with an Elliptic Inclusion under Tension, Transactions of the Japan Society of Mechanical Engineers, (Version A), Vol.55, No.511, pp.515-522, 1989.
[22] Hatta, M., Murakami, T., and Ishida, M.: Stress Field due to Interference between Two Elliptical Inclusions, Transactions of the Japan Society of Mechanical Engineers, Vol.464, pp.1057-1065, 1985.
[23] Hasebe, N., Ueda, M., Yamamoto, Y., and Nakamura, T.: Analytical Study about the Fracture Mechanism around the Inclusion with Angular Corners, Journal of Structural Engineering, Vol.3 A, pp.369-382, 1992.
[24] Nakane, J.: Interference Problem of Rhombic Rigid Inclusions, Graduate dissertation, Nagoya Institute of Technology, 1992.
[25] Ziegeldorf, S.: Fracture Mechanics Parameters of Hardened Cement Paste, Aggregates, and Interfaces, in Fracture Mechanics of Concrete, ed. Wittmann, F.H., Elsevier, pp.371-409, 1983.
[26] Saito, M.: Characteristics of Microcracking in Concrete under Static and Repeated Tensile Loading, Cement and Concrete Research, Vol.17, pp.211-218, 1987.

[27] Wolinski, S., Hordijk, D.A., Reinhandt, H.W., and Cornelissen, H.A.W.: Influence of aggregate Size on Fracture Mechanics Parameters of Concrete, Int. J. of Cement Composites and Lightweight Concrete, Vol.9, NO.2, pp.95-103, 1987.
[28] Yamamoto, Y., Ueda, M., Hasebe, N., and Nakamura, T.: Stress Analysis of Cracks and Debonding Generated by Inclusions, Collection of Papers for the 41st Applied Mechanics Union Lecture, pp.271-272, 1992.
[29] Nakanishi, H., Umagawa, S., Akazaki, T., and Suzuki M.: Stress Intensity Factors of Interface Cracks around a Circular Inclusion, Transactions of the Japan Society of Mechanical Engineers, (Version A), Vol.52, No.479, pp.1655-1662, 1986.
[30] Nakanishi, H., Kitazawa, M., Iwamoto, S., and Suzuki, M.: Progress of Interface Debonding and Cracking in Composite Materials, Transactions of the Japan Society of Mechanical Engineers, (Version A), Vol. 47, pp 990 to 997, 1981
[31] Nakanishi, H., Umagawa, S., and Suzuki, M.: Stress Intensity Factors of Interface Cracks around an Elliptical Rigid Inclusion, Transactions of the Japan Society of Mechanical Engineers, (Version A), Vol. 55, No. 516, pp 1756 to 1762, 1989
[32] Saito, M., Kaseba, S., and Kawamura, M.: The Tensile Strength Characteristics of Concrete as a Composite Material, Journal of the Japan Society for Composite Materials, Vol. 6, pp 16 to 22, 1980
[33] Ueda, M., Hasebe, N., Kojima, K., and Nakamura, T.: Fracture Mechanics Study on Properties of the Debonding Propagation at the Interface of the Rhombic Rigid Inclusion, Journal of Structural Mechanics and Earthquake Engineering, No. 455/I-21, pp 45 to 54, 1992
[34] Murakami, Y. et al.: Stress Intensity Factors Handbook, Pergamon Press, Oxford, 1987
[35] Zaitsev, Y.: Crack Propagation in a Composite Material, Fracture Mechanics of Concrete, ed. by Wittmann, F.H., Elsevier, Amsterdam, pp 251 to 299, 1983
[36] Yoshimoto, A.: Deformation and Fracture of Concrete, Gakken Publishing Co., Ltd., pp 64 to 66, 1990
[37] Watanabe, N. and Hashiba, M.: Study on Tensile Strength of Concrete, Review of the General Meeting/Technical Session, Vol. 38, pp 294 to 297, 1984
[38] Yoshimoto, A., Hasegawa, H., and Kawakami, M.: Study of Tensile Creep Mechanism, Review of the General Meeting/Technical Session, Vol. 36, pp 333 to 336, 1982
[39] Yoshimoto, A. and Kawakami, M.: Micro Cracks in Cement Paste by Flexural Tensile Strength, Review of the General Meeting/Technical Session, Vol. 26, pp 275 to 277, 1972
[40] Carino, N.J. and Slate, F.O.: Limiting Tensile Strain Criterion for Failure of Concrete, ACI Journal, March, pp 160 to 165, 1976
[41] Iida, J., Hasebe, N., and Nakamura, T.: Approximate Expressions for SIF of Crack Initiating from Notch for Thin Plate Bending and Plane Problems, Engrg.Fract. Mech., Vol.36, No.5, pp 819 to 825, 1990
[42] Ishida, M. and Noguchi, H.: Problem of Load Inside Infinite Body with Round Inclusions and Arbitrary Group of Cracks, Transactions of the Japan Society of Mechanical Engineers, (Version A), Vol. 49, No. 438, pp 147 to 155, 1983
(Accepted June 18)